IEEE Access
Multidisciplinary ⋮ Rapid Review ⋮ Open Access Journal

Received November 1, 2021, accepted December 10, 2021, date of publication December 14, 2021, date of current version December 31, 2021.

Digital Object Identifier 10.1109/ACCESS.2021.3135495

An Air Target Tactical Intention Recognition Model Based on Bidirectional GRU With Attention Mechanism

FEI TENG, XINPENG GUO, YAFEI SONG, (Member, IEEE), AND GANG WANG
Air and Missile Defense College, Air Force Engineering University, Xi'an 710051, China

Corresponding authors: Xinpeng Guo (xinpeng_guo@163.com) and Yafei Song (yafei_song@163.com)

This work was supported in part by the National Natural Science Foundation of China under Grant 61703426 and Grant 72001214; in part by the Young Talent fund of University Association for Science and Technology, Shaanxi, China, under Grant 2019038; and in part by the Innovation Capability Support Plan of Shaanxi, China, under Grant 2020KJXX-065.

ABSTRACT Traditional aerial target tactical intention recognition is based on a single moment of reasoning, while actual battlefield target tactical intention is realized by a series of actions, so the target state reflects dynamic and temporal variation. To solve this problem, bidirectional propagation and attention mechanisms are introduced based on a gated recurrent unit (GRU) network, and bidirectional gated recurrent units with attention mechanism (BiGRU-Attention) air target tactical intention recognition model is proposed. We use a hierarchical approach to construct the air combat intention characteristic set, encode it into temporal characteristics, encapsulate the decision-maker's experience into labels, learn the deep-level information in the air combat intention characteristic vector through a BiGRU neural network, and use the attention mechanism to adaptively assign network weights, and then place air combat characteristic information with different weights in a softmax function layer for intention recognition. Comparison with a traditional air tactical target intention recognition model and analysis of ablation experiments show that the proposed model effectively improves the tactical intention recognition of air targets.

INDEX TERMS Intention recognition, attention mechanism, bidirectional GRU, temporal variation, aerial targets.

I. INTRODUCTION

In the modern, information-based air battlefield, the vigorous development of aviation science and military technology has led to increasing threats to air targets. At the same time, the complexity of the battlefield environment and information asymmetry continues to increase due to the continuous application of high technology, making it difficult to accurately identify the enemy's target intentions in real-time based only on experience. Hence intelligent reasoning methods are needed [1].

Research on intention recognition has been conducted in the military field to meet the needs of operational decision systems. Studies of the intention recognition of enemy targets in complex battlefield environments include the areas of evidence theory [2], template matching [3], expert systems [4], Bayesian networks [5]–[7], and neural networks [8]–[12]. Zhao *et al.* [2] used vessels sensors to measure the characteristic information of an air target and establish a confidence rule base. Thus the target intention was identified by fusing multiple sources of information using evidential inference. Li [3] designed an intention recognition reasoning model on a template based on a situational database and proposed an intention recognition template matching method based on D-S evidence theory. Yin *et al.* [4] used domain expert knowledge to construct a knowledge base, expressed relationships between battlefield situations and combat intentions in the form of rules, and obtained a result based on an inference engine. Qing *et al.* [5], Song *et al.* [6], and Xue *et al.* [7] determined Bayesian network parameters based on military expert knowledge, using nodes, directed arcs, and conditional probabilities to represent characteristics, transfer relationships, and relationship strengths, respectively. New events have been used to influence backward propagation to update network parameters until an intention exceeds a threshold

The associate editor coordinating the review of this manuscript and approving it for publication was Seok-Bum Ko.

value, which is the identified intention. References [2]–[7] have achieved certain results in intention recognition based on different methods. However, the construction of the probability distribution function of D-S evidence theory and the collection of evidence information; the construction of template matching technology standard template library; the establishment of expert system inference engine and knowledge base; the determination of the Bayesian network structure and probability distribution parameters all need to organize, abstract and explicitly describe the knowledge and experience of the domain experts, and it is very difficult to implement the project and express the knowledge [13].

Wu [8] used Recurrent Neural Network (RNN) to study the intent of aerial cluster targets. Zhou *et al.* [9] used long short-term memory (LSTM) to repair incomplete air combat information, and used a decision tree to reason about target intentions. Ou *et al.* [10] used a semi-supervised learning method to identify the intention of an enemy airborne target, and improved the accuracy of intention recognition through pre-training. Zhai *et al.* [11] proposed an air combat target threat assessment method based on a standardized fully connected residual network. The batch normalization algorithm is used to improve the convergence speed of the model, and the residual network is used to enhance the network learning ability, which effectively improves the accuracy of intention recognition. Wei *et al.* [12] proposed a target intention recognition model based on radial basis function (RBF) neural network. References [8]–[12] collected battlefield information, selected appropriate characteristics, and preprocessed data to obtain a dataset, which was input to a neural network, using its adaptive and self-learning capabilities to obtain combat intention recognition rules used to deduce an enemy's intention. However, by relying on the characteristic information of a single moment for analysis and reasoning, the above methods have difficulty finding the hidden deep information from the target state characteristic of temporal variation.

In the battlefield, target intention is implemented through a series of tactical actions, so the dynamic attributes of the target and the battlefield environment will present characteristics of dynamic and temporal variation. Combat actions will be deceptive and covert, and it is not scientific enough to reason based on a single moment. Aiming at the temporal characteristics, Ou *et al.* [13] proposed an intelligent target tactical intention recognition model based on a long short-term memory (LSTM) network, which well recognizes target combat intentions and conforms to temporal characteristics and logical relationships. Xue *et al.* [14] proposed an air target intent recognition method based on Panoramic Convolutional Long Short-Term Memory Neural Network (PCLSTM), which uses PCLSTM to improve feature learning capabilities, and designs a time series pooling Layer to reduce the number of neural network parameters. The above two air target intention recognition methods based on LSTM have good results, but they can only use historical moment information to make judgments on current information, and cannot use future moment information. In addition, decision-makers will focus on key features when judging the intentions of enemy air targets, especially when different types of features map different intentions, they should increase the weight of key features.

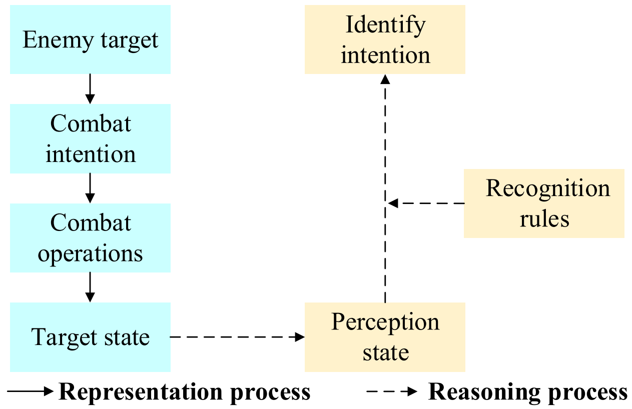

FIGURE 1. Hierarchical representation and reasoning process of intention.

In order to effectively solve the shortcomings of the above methods and improve the efficiency of air target intention recognition, we propose an air target intent recognition method based on bidirectional gated recurrent units with attention mechanism (BiGRU-Attention). The main innovations are as follows:

1) We use a hierarchical strategy to extract features related to air target intent recognition from three aspects, and reasonably encode non-numerical features.

2) In order to improve the speed of air target intent recognition, we use gated recurrent unit (GRU) as the basic network. Compared with LSTM, GRU has similar performance but simpler structure, so the use of GRU can effectively reduce the time complexity of air target intent recognition.

3) The bidirectional propagation mechanism is introduced to join the GRU network. Compared with GRU, bidirectional gated recurrent unit (BiGRU) can make full use of historical and future information to form comprehensive judgment and improve network learning ability.

4) The attention mechanism is introduced to simulate the automatic attention ability of decision-makers for key features. The attention mechanism adaptively pays attention to key features by assigning weights to features to improve the accuracy of intention recognition.

II. PROBLEM DESCRIPTION OF AIR TARGET INTENTION RECOGNITION

Air target tactical intention is the process of reasoning about the operational intention of enemy targets in a real-time, adversarial environment by extracting information in the corresponding space-time domain, static attributes, and real-time dynamic information for analysis, and combining this with military knowledge of the domain [15]. The process is shown in Figure 1.

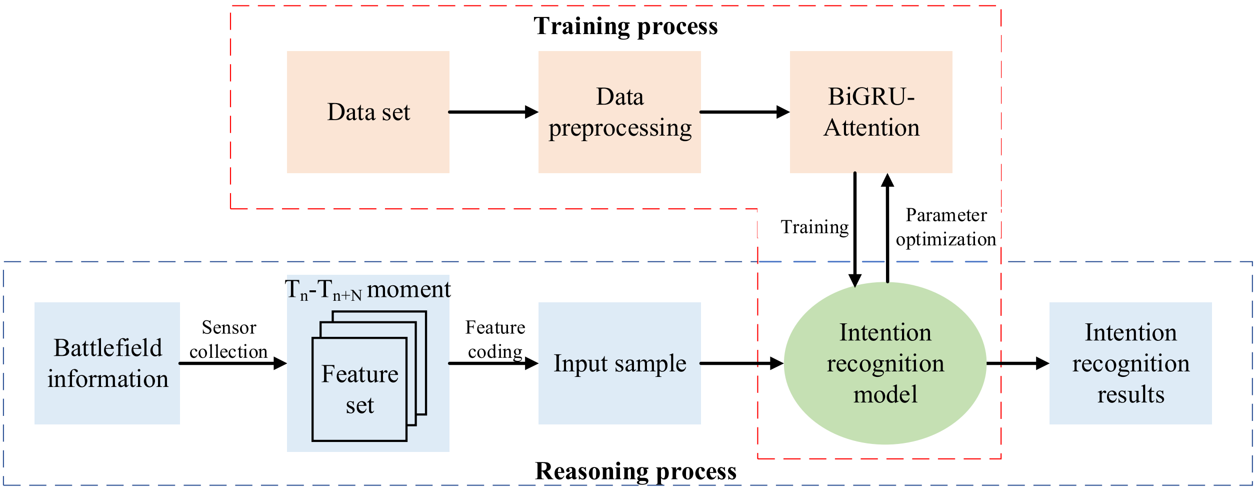

FIGURE 2. Process of air target tactical intention recognition. The red frame is the training process, and the blue frame is the Reasoning process.

This is a typical pattern recognition problem that can be described as a mapping of air combat intention recognition characteristics to air combat intention types. Define $\boldsymbol{I} = (i_1, i_2, \cdots, i_n)$ as the air target tactical intention space, and $\boldsymbol{V}^t$ as the real-time characteristic information on the battlefield at time t. The target will attempt to deceive our decision-makers and cause wrong judgments, so the enemy's predicted operational intention based on a single moment will differ significantly from reality. It is more scientific to infer this from information at multiple consecutive moments. Define $\boldsymbol{V}_T$ as a temporal characteristic set composed of characteristic sets from t_1 to t_T at T consecutive moments. We can determine the mapping from the tactical intention space $\boldsymbol{I}$ to the temporal characteristic set $\boldsymbol{V}_T$ as

$$\boldsymbol{I} = f\left(\boldsymbol{V}_T\right) = f\left(\boldsymbol{V}^{(t_1)}, \boldsymbol{V}^{(t_2)}, \cdots, \boldsymbol{V}^{(t_T)}\right) \tag{1}$$

Due to the high confrontation, uncertainty, and complexity of air warfare, it is difficult to inductively derive a mapping relationship from tactical intention types to temporal characteristic sets through formulas [13]. We train the BiGRU-Attention network structure using the air combat dataset, so as to implicitly establish a mapping relationship from the tactical intention type to the temporal characteristic set, as shown in Figure 2.

In the process of air target tactical intention recognition, a training dataset is obtained through intention type calibration of historical data by air combat experts. The preprocessed dataset is input to the BiGRU-Attention network for training to obtain the mapping relationship between the air combat intention type and the temporal characteristic set. In actual air combat, state information of the target is collected by sensors in real-time at N successive moments T_n to T_{n+N}. This information is integrated and coded in the trained target intention recognition model.

We assume: (1) environmental conditions such as terrain, atmosphere, and climate are approximately the same for both sides; and (2) the enemy air target tactical intention does not change in the extracted temporal series [1].

A. SPATIAL DESCRIPTION OF TARGET TACTICAL INTENTION

The target tactical intention space has intention spaces for different combat forms, scenarios, and entities. It is necessary to define a tactical intention space suitable to the combat situation. Zhao *et al.* [2] defined the tactical intention space for enemy air targets against our surface naval vessels as {reconnaissance, surveillance, attack, cover}; Chen *et al.* [16] established the tactical intention space for a single group of enemy fleet formations as {attack, reconnaissance, evasion, cover}; Zhang *et al.* [17] defined the tactical intention space for enemy air targets against our submarines as {attack, submarine search, repel, patrol}; and Lu *et al.* [18] established the tactical intention space as {attack, evasion, patrol} for underwater threat targets. With an airspace unmanned aerial vehicle (UAV) engagement as the research object, we establish the tactical intention space of the enemy target as {surprise, feint, attack, reconnaissance, retreat, surveillance, electronic interference}.

The key to applying BiGRU-Attention models to tactical intention recognition is to convert human cognitive patterns to labels trained by intelligent models and corresponding to intention types. Analyzing the process of decision-makers inferring the tactical intentions of enemy targets, it can be seen that it is difficult for decision-makers to express the process of judgment of the enemy's target intentions through simple formulas after obtaining battlefield situation information and combining their own experience. However, human cognitive experience is often implicit in the inference process of the enemy's combat intentions. Therefore, the cognitive experience of decision-makers can be encapsulated into labels to train the BiGRU-Attention model [19]. Figure 3 shows the combat intention type encoding and

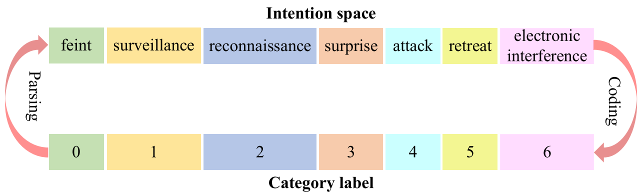

FIGURE 3. Schematic diagram of combat intention coding and analysis. The same color is a set of correspondence.

pattern resolution mechanisms for the target combat intention types established in this paper. For example, an intention recognition result of 4 indicates an attack intention. Hence the coding of enemy combat intention can simply and clearly express the cognitive experience of decision-makers, making it easier to train the model.

B. CHARACTERISTIC DESCRIPTION OF AIR TARGET TACTICAL INTENTION RECOGNITION

The enemy target tactical intention is highly correlated with its threat level and combat mission. For example, an enemy facing a threat level much greater than it poses is not likely to attack. Therefore, identifying enemy threat levels and combat missions requires the extraction of different air combat characteristics.

Many factors affect the threat level of a target. We consider the distance, speed, angle, and flight acceleration between the enemy and our side. As shown in Figure 4.

The air combat capability factor is also an important factor that affects the degree of target threat. For the air combat capability of a fighter, a single-air combat capability threat function is constructed according to the reference [20].

$$C = \left[ln\varepsilon_1 + ln\left(\varepsilon_2 + 1\right) + ln(\sum \varepsilon_3 + 1)\right]\varepsilon_4\varepsilon_5\varepsilon_6\varepsilon_7 \quad (2)$$

where ε_1 to ε_7 respectively represent fighter maneuverability; airborne weapon performance; airborne equipment detection capability; the fighter's flight, operational, and combat survival performance; and electronic information countermeasure performance. The air combat capability threat is inherent to fighters, so the associated factors of various fighters of both sides in a certain period can be calculated and saved in the database, whose data are updated in real-time.

When an enemy fighter performs a certain combat mission, its characteristic information must meet certain conditions. For example, fighters usually approach targets at high speed, and their flight speeds are generally 735km/h to 1470km/h. Low-and high-altitude penetration corresponds to heights of 50m to 200m and, 10000m to 11000m respectively [14]. The target radar signal status is also related to combat missions. For example, air-to-air radars are usually kept on during air combat, and air-to-air radars and marine radars are kept on during reconnaissance missions. Different aircraft types have different application values and tactical meanings. Fighters are more aggressive and reconnaissance aircraft have

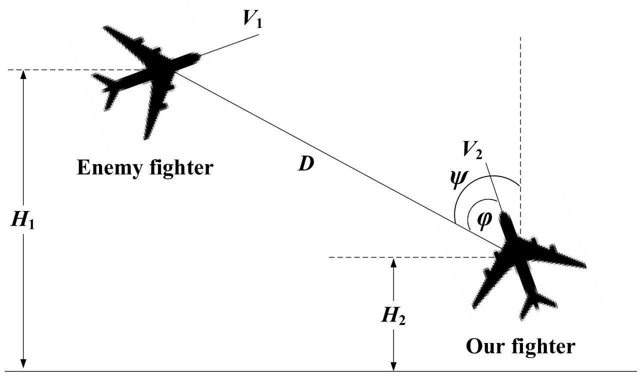

FIGURE 4. Relative geometric position of air combat. (H1, H2 are the flight altitudes of the enemy and our; V1, V2 are the flight speeds of the enemy and our; D is the distance between the two parties; ψ is the heading angle; φ is the azimuth angle).

strong reconnaissance capabilities. Therefore, enemy aircraft types can also be used as tactical intention identification characteristics.

In addition, air target tactical intentions are closely related to fighter maneuvers. There are two types of common maneuver library designs: one is a "typical tactical maneuver library" designed based on typical air combat tactical aircraft actions, and the other is a "basic maneuver library" designed based on basic air combat maneuvers. Since we are studying time sequence characteristics, we collect 12 frames of target characteristic information for tactical intent recognition, and the control algorithm of the "typical tactical maneuver library" is complicated to solve, and it is difficult to determine the exit and transition time of the action, so we do not use it. The "basic maneuvering library" [21] was proposed by NASA scholars based on the most commonly used maneuvers in air combat, mainly including {maximum acceleration, maximum deceleration, maximum overload climb, maximum overload dive, maximum overload right turn, maximum overload left turn, stable fractal} 7 maneuvers, but the maneuvers combined by these seven maneuvers are not enough, and the use of extreme maneuvers is obviously not in line with the reality of air combat. We use 11 "improved basic maneuver library" [22], {even forward flight, deceleration forward flight, acceleration forward flight, climb, right climb, left climb, dive, right dive, left dive, right turn, left turn}.

In summary, the air target tactical intention recognition characteristic set in this paper is a 17-dimensional characteristic vector, {air-to-air radar status, marine radar status, jamming status, jammed status, maneuver type, enemy aircraft type, enemy aircraft acceleration, enemy aircraft altitude, enemy aircraft speed, enemy aircraft air combat capability factor, heading angle, azimuth angle, our aircraft acceleration, our aircraft altitude, our aircraft speed, our aircraft air combat capability factor, the distance between the two sides}. The characteristic description diagram is shown in Figure 5 and can be divided into numeric and non-numeric characteristics.

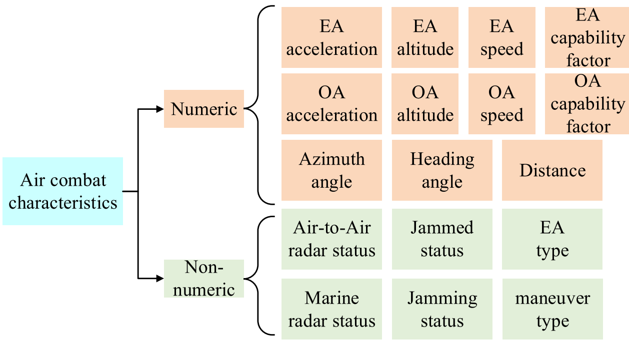

FIGURE 5. Characteristic set of the tactical intention of the aerial target. EA and OA are abbreviations for enemy aircraft and our aircraft.

III. AIR COMBAT INTENTION RECOGNITION MODEL BASED ON BIGRU-ATTENTION

The BiGRU-Attention model has three layers: air combat characteristic vector input, hidden, and output. The hidden layer consists of BiGRU, attention, and dense layers. The network input node input = (12,17), and output node output = 7, where 12 is the timestep, 17 is the number of characteristic dimensions, and 7 is the number of intention categories. Figure 6 shows the structure of the model.

A. INPUT LAYER

The input layer preprocesses collected air combat characteristic datasets to obtain a characteristic vector that the BiGRU layer can directly accept and process. The following is a detailed description of the normalization of numerical data, the encoding of non-numerical data, and the construction of samples.

1) Normalize the numeric air combat characteristic data to eliminate the influence of data dimensions and improve the efficiency of network convergence. We normalize 11 types of numerical air combat characteristic data such as enemy aircraft acceleration, our aircraft acceleration, and heading angle. For the x-th numeric data, $\boldsymbol{F}_x = [f_{x1}, f_{x2}, \cdots f_{xi}, \cdots, f_{xn}]$ $(x = 1, 2, \cdots, 11)$, n is the total number of data points. The mapping of the i-th original data value f'_{xi} of the x-th kind to the interval [0,1] is

$$f'_{xi} = \frac{f_{xi} - min\boldsymbol{F}_x}{max\boldsymbol{F}_x - min\boldsymbol{F}_x} \tag{3}$$

where $min\boldsymbol{F}_x$ and $max\boldsymbol{F}_x$ are the minimum and maximum values, respectively, of $\boldsymbol{F}_x$.

2) Encode non-numeric air combat characteristic data. The codes of the air-to-air radar, marine radar and interference states take the values 0 and 1. For example, in the air-to-air radar state, 0 means the radar is off, and 1 means it is on. For the attribute data of maneuver type and enemy aircraft type, Miller 9-level quantization theory [23], [24] is applied to obtain the coded data of non-numeric characteristics. Coded data are then normalized.

3) Construct training samples and test samples according to the following methods. Assuming that the characteristic data of the previous 12 moments are used to identify the intention of the enemy aircraft during this period of time, the function mapping relationship is as follows:

$$Q_1 = f\left(\boldsymbol{v}_1, \boldsymbol{v}_2, \cdots, \boldsymbol{v}_{11}, \boldsymbol{v}_{12}\right) \tag{4}$$

where Q_1 represents the type of intention identified in the time period 1 to 12; $\boldsymbol{v}_i$, $i \in (1, 2 \cdots, 12)$ represents the historical characteristic data at the i-th time. Select $(\boldsymbol{v}_1, \boldsymbol{v}_2, \cdots, \boldsymbol{v}_{11}, \boldsymbol{v}_{12})$ as the first set of input data, and label the intent type q_1 corresponding to the time period 1 to 12; use $(\boldsymbol{v}_2, \boldsymbol{v}_3, \cdots, \boldsymbol{v}_{12}, \boldsymbol{v}_{13})$ as the second set of input data, the label is the intent type q_2 corresponding to the time period 2 to 13. By analogy, the training sample input data and training sample label are composed as shown in (5) (6). The method of constructing the test data is consistent with the training sample data [25].

$$\begin{bmatrix} \boldsymbol{v}_1 & \boldsymbol{v}_2 & \cdots & \boldsymbol{v}_m \\ \boldsymbol{v}_2 & \boldsymbol{v}_3 & \cdots & \boldsymbol{v}_{m+1} \\ \vdots & \vdots & \ddots & \vdots \\ \boldsymbol{v}_{11} & \boldsymbol{v}_{12} & \cdots & \boldsymbol{v}_{m+10} \\ \boldsymbol{v}_{12} & \boldsymbol{v}_{13} & \cdots & \boldsymbol{v}_{m+11} \end{bmatrix} \tag{5}$$

$$\begin{bmatrix} q_1 & q_2 & \cdots & q_n \end{bmatrix} \tag{6}$$

B. HIDDEN LAYER

1) BIDIRECTIONAL GATED RECURRENT UNITS LAYER

As a variant of Recurrent Neural Network (RNN), the Gated Recurrent Unit (GRU) also has a recursive structure similar to RNN, and has a "memory" function to process time-series data. At the same time, GRU can effectively alleviate the problems of gradient disappearance and gradient explosion that may occur in the RNN training process, and effectively solve the problem of long-term memory. The Long Short Term Memory (LSTM) network is also a variant of RNN, which is similar to GRU in performance, but GRU is simpler in structure, which can reduce the amount of computation and improve training efficiency [26], [27]. The internal structure of the GRU is shown in Figure 7.

GRU has two inputs, which are the output state at the previous moment $\boldsymbol{h}_{t-1}$ and the input sequence value $\boldsymbol{x}_t$ at the current moment, and the output is the state at the current moment $\boldsymbol{h}_t$. It mainly updates the state of the model by resetting the gate $\boldsymbol{r}_t$ and updating the gate z_t. The reset gate controls the degree to which historical state information is forgotten so that the network can discard unimportant information. The update gate z_t controls the proportion of the previous state information brought into the current state, helping the network to remember long-term information [28]. These are calculated as:

$$\begin{cases} \boldsymbol{r}_t = \sigma\left(\boldsymbol{W}_r \boldsymbol{x}_t + \boldsymbol{U}_r \boldsymbol{h}_{t-1}\right) \\ z_t = \sigma(\boldsymbol{W}_z \boldsymbol{x}_t + \boldsymbol{U}_z \boldsymbol{h}_{t-1}) \\ \tilde{\boldsymbol{h}}_t = \tanh(\boldsymbol{W}_{\tilde{h}} \boldsymbol{x}_t + \boldsymbol{U}_{\tilde{h}}(\boldsymbol{r}_t \odot \boldsymbol{h}_{t-1})) \\ \boldsymbol{h}_t = (1 - z_t) \odot \boldsymbol{h}_{t-1} + z_t \odot \tilde{\boldsymbol{h}}_t \end{cases} \tag{7}$$

In the formula and figure 7, σ is the sigmoid activation function, which is used to transform the intermediate state to

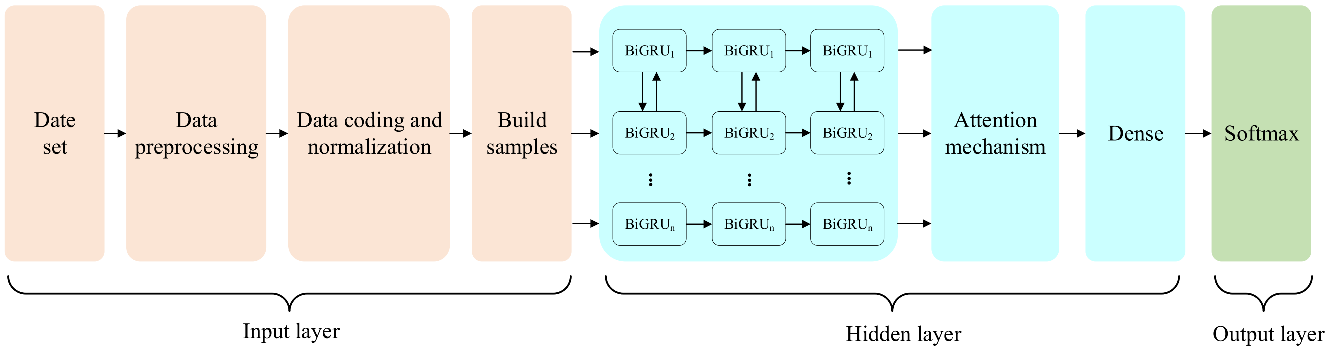

FIGURE 6. **BiGRU-Attention model. The input of the model is the characteristic set of the tactical intention of the air target, and the output is the label of the type of the model's recognition.**

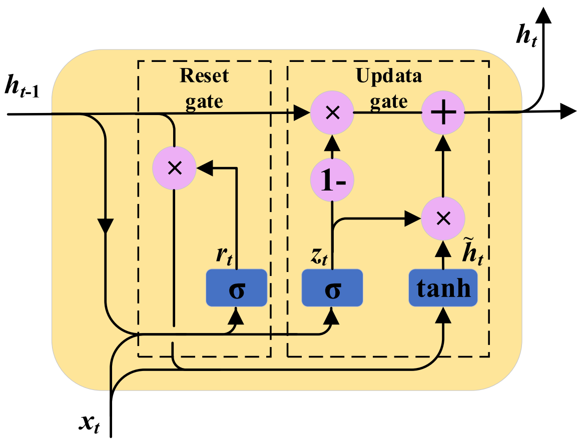

FIGURE 7. **GRU Internal computing structure.**

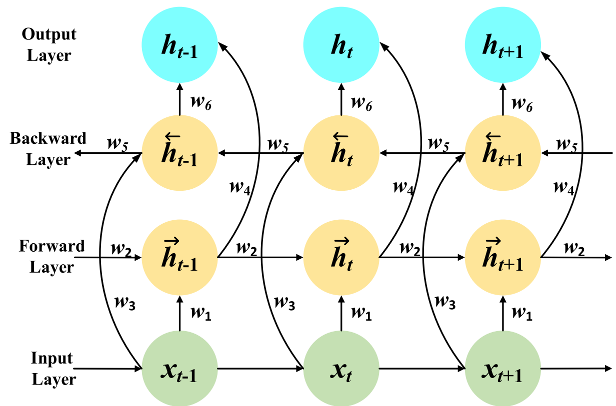

FIGURE 8. **Bidirectional GRU network structure.**

the range of [0,1]; $\boldsymbol{h}_{t-1}$ and $\boldsymbol{h}_t$ are the output states at the time (t-1) and time t respectively; $\boldsymbol{x}_t$ is the input sequence value at time t; $\tilde{\boldsymbol{h}}_t$ is the candidate output state; $\boldsymbol{W}_r$, $\boldsymbol{W}_z$, $\boldsymbol{W}_{\tilde{h}}$, $\boldsymbol{U}_r$, $\boldsymbol{U}_z$ and $\boldsymbol{U}_{\tilde{h}}$ are the corresponding weight coefficient matrices of each part; tanh is a hyperbolic tangent function; $\odot$ is the Hadamard Product of the matrix.

The traditional GRU structure usually propagates in a single direction along the direction of sequence transmission. The information obtained by it is historical information before the current time, which leads to the neglect of future information. The BiGRU structure is composed of forward GRU and backward GRU, which has the function of capturing the information characteristics before and after. The model structure is shown in Figure 8.

It can be seen from Figure 8 that the hidden layer state h_t of BiGRU at time t can be obtained through the forward hidden layer state $\vec{h}_t$ and the backward hidden layer state $\overleftarrow{\boldsymbol{h}}_t$. The forward hidden layer state $\vec{\boldsymbol{h}}_t$ is determined by the current input $\boldsymbol{x}_t$ and the forward hidden layer state $\vec{\boldsymbol{h}}_{t-1}$ at the time (t-1). The backward hidden layer state $\overleftarrow{\boldsymbol{h}}_t$ is determined by the current input $\boldsymbol{x}_t$ and the backward hidden layer state $\overleftarrow{\boldsymbol{h}}_{t+1}$ at time ($t+1$) [29]. These are calculated as

$$\vec{\boldsymbol{h}}_t = f\left(\boldsymbol{w}_1\boldsymbol{x}_t + \boldsymbol{w}_2\vec{\boldsymbol{h}}_{t-1}\right) \tag{8}$$

$$\overleftarrow{\boldsymbol{h}}_t = f\left(\boldsymbol{w}_3\boldsymbol{x}_t + \boldsymbol{w}_5\overleftarrow{\boldsymbol{h}}_{t+1}\right) \tag{9}$$

$$\boldsymbol{h}_t = g\left(\boldsymbol{w}_4\vec{\boldsymbol{h}}_t + \boldsymbol{w}_6\overleftarrow{\boldsymbol{h}}_t\right) \tag{10}$$

where $\boldsymbol{w}_i$, $i \in (1, 2 \cdots, 6)$ are the weights of each layer.

2) ATTENTION MECHANISM LAYER

The attention mechanism is similar to the brain signal processing of human vision. It highlights characteristics that account for a greater proportion of prediction results by calculating the weights of characteristic vectors output from BiGRU at different moments, enabling better performance. The attention mechanism performs well with temporal data such as machine translation and speech recognition. It has a relatively good effect on classification prediction. It can be used alone or as a layer of other hybrid models [30]. In air target tactical intention recognition, the neural network uses the Attention mechanism to focus on some key characteristics during the training process, the core of which is the weight coefficient [31]. By learning the importance of each characteristic, and then assigning a corresponding weight to each characteristic according to the importance. For example, if the enemy aircraft's intention is to attack, then characteristics such as heading angle and maneuver type will be assigned more weight to deepen the model memory. The

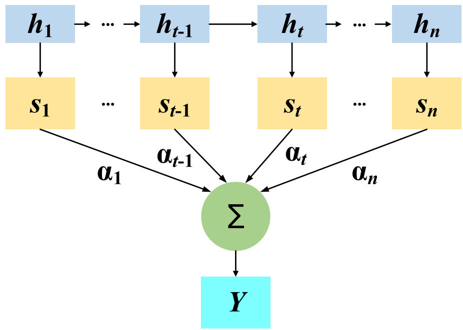

FIGURE 9. **Attention mechanism structure. The input of the attention mechanism is the output of BiGRU, and the output is the set of weights.**

structure of the attention mechanism is shown in Figure 9. $\boldsymbol{h}_t$ is the t-th characteristic vector output by BiGRU, which is input to the hidden layer of the attention mechanism to obtain the initial state vector $\boldsymbol{s}_t$, multiplied by the weight coefficient α_t, and accumulated and summed to obtain the final output state vector $\boldsymbol{Y}$. The calculation formulas are

$$\boldsymbol{e}_t = tanh(\boldsymbol{w}_t\boldsymbol{s}_t + \boldsymbol{b}_t) \tag{11}$$

$$\alpha_t = \frac{exp(\boldsymbol{e}_t)}{\sum_{i=1}^{t} \boldsymbol{e}_i} \tag{12}$$

$$\boldsymbol{Y} = \sum_{t=1}^{n} \alpha_t \boldsymbol{s}_t \tag{13}$$

where $\boldsymbol{e}_t$ is the energy value determined by the state vector $\boldsymbol{s}_t$ of the t-th eigenvector; $\boldsymbol{w}_t$ is the weight coefficient matrix of the t-th eigenvector, and $\boldsymbol{b}_t$ is the offset corresponding to the t-th eigenvector. According to formula (12), the conversion from the initial input state to the new attention state can be realized, and the final output state vector $\boldsymbol{Y}$ is obtained through formula (13). Finally, Y and the dense layer are integrated and output to the final output layer.

C. OUTPUT LAYER

The input of the output layer is the output of the attention mechanism layer in the hidden layer. We use the multi-class softmax function to calculate and get the intention classification result. The calculation formula is

$$y_k = \mathrm{softmax}\,(\boldsymbol{w}\boldsymbol{Y} + \boldsymbol{b}) \tag{14}$$

where $\boldsymbol{w}$ is the weight coefficient matrix to be trained from the attention mechanism layer to the output layer, $\boldsymbol{b}$ is the corresponding bias to be trained, and y_k is the output prediction label of the output layer.

IV. EXPERIMENTAL ANALYSIS

A. EXPERIMENTAL DATASET

The experiment took a certain airspace UAV engagement as the research background, whose data came from a combat simulation system. We ran the simulation several times to obtain a variety of air combat intention modes, from which 10,000 air combat intention samples were randomly selected. Twelve consecutive frames of information were collected for each sample, where each frame included 17 dimensions of information such as heading angle, flight height, interference status, and radar status. Due to a large amount of data in the sample set, experts at air combat were chosen to compile intention recognition rules to generate intention labels. Pattern classification of air combat intention samples was performed by the computer, and sample data with intention classification ambiguities were revised by experts. The dataset included seven target tactical intentions, including 21.6% attack, 20.0% penetration, 19.8% reconnaissance, 12.9% surveillance, 10.0% feint, 9.25% electronic jamming, and 6.45% retreat. The sample size was 10000, with training and test sets in 8:2 proportion, that is, 8000 for training and 2000 for testing.

B. EXPERIMENTAL SETTINGS

We use deep learning framework Keras 2.4.3 and programing language Python 3.8 on an x86-64 CentOS7 PC, which is based on Intel® Xeon(R) Sliver 4110 CPU @2.10GHz, 64G RAM, and Quadro RTX 5000/PCle/SSE2 GPU with CUDA 11.0 accelerating computation.

In the experiment, many hyper-parameters need to be set and adjusted, and adjusted according to the accuracy. Record the number of hidden layers is HL, and the number of nodes in each hidden layer is HS. (1) Keep the number of hidden layers unchanged, set different hidden layer nodes respectively, analyze the influence of the number of hidden layers nodes on the performance of the model. Set HL=1, HS=[64], [128], [256], [512], and get the optimal number of hidden layer nodes. The results are shown in Figure 10 (a). (2) According to the optimal number of nodes of the hidden layer obtained in (1), set different hidden layer numbers under the condition that the overall number remains unchanged, and analyze the influence of hidden layer number on the performance of the model, set HL=1, HS=[256]; HL=2, HS=[128,128]; HL=3, HS=[128,64, 64]; HL=4, HS=[128,64,32,32], the results are shown in Figure 10 (b). (3) The optimal optimizer is selected from five optimizers of Nadam, Adam, Adagrad, Adadela, and Rmsprop, and the result is shown in Figure 10 (c). (4) Set the Nadam learning rate as 0.002, 0.004, 0.006, 0.008, and 0.010, and select the most appropriate learning rate from them. The result is shown in Figure 10 (d).

From Figure 10 (a) (b), it can be seen that the number of hidden layer nodes and hidden layers is not the more the better, but there is a suitable number. If there are too many hidden layer nodes, the phenomenon of "Overfitting" will easily occur. In the case of a single hidden layer, the number of hidden layer nodes is gradually increased, and 256 is the optimal number of hidden layer nodes. In the case that the total number of hidden layer nodes remains unchanged, increasing the network depth appropriately will effectively improve the accuracy of model recognition, but when the number of layers reaches three, the effect of increasing the number of hidden layers will become worse. It can be seen from Figure 10 (c) (d) that among the five optimizers, the Nadam optimizer performs best, and by gradually increasing

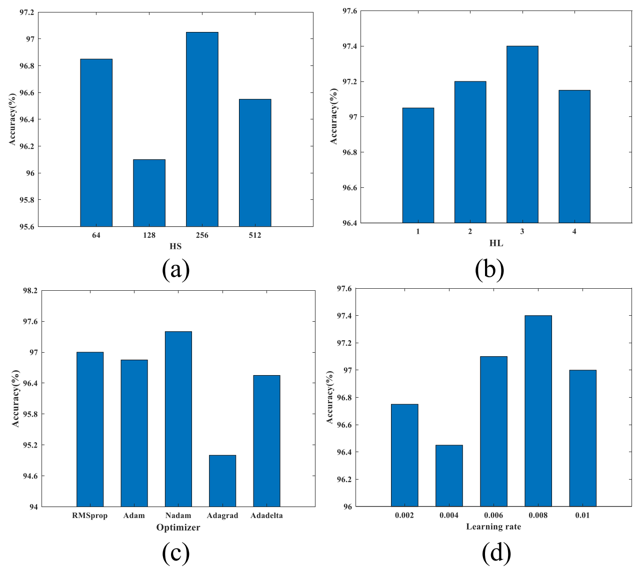

FIGURE 10. Model parameter setting experiment result figure. (a) Influence of the number of hidden layer nodes on model performance. (b) Influence of the number of hidden layers on model performance. (c) Influence of the optimizer on model performance (d) Influence of learning rate on model performance.

TABLE 1. Model experimental parameters.

Parameter	Value
Loss function	Categorical_crossentropy
Optimizer	Nadam
Hidden layer	3
Hidden neuron	128、64、64
Batch size	128
Dropout	0.5
Epoch	200
Learning rate	0.008

its learning rate, 0.008 is the optimal learning rate. Other key hyperparameter settings are shown in Table 1.

C. BIGRU-ATTENTION MODEL RECOGNITION RESULT ANALYSIS

After training, the BiGRU-attention model was tested on 20% of the samples. Experiments showed that the accuracy of the proposed network model reached 97.4%. To further observe the relationship between recognition intentions, a confusion matrix was designed, whose diagonal line indicates the number of correctly identified samples, as shown in Figure 11.

It can be seen from Figure 11 that the model had high recognition accuracy for all seven kinds of intention recognition; in particular, the retreat intention recognition accuracy could reach 100%. A small percentage of attack intentions were misidentified as feint intentions, and a small percentage of reconnaissance and surveillance intentions were misidentified as each other. After analysis, we found that the air combat characteristics corresponding to the two intentions were similar, making the intentions more

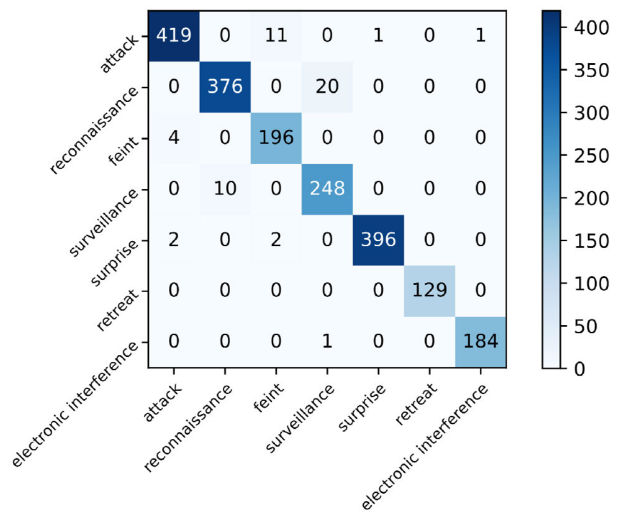

FIGURE 11. Confusion matrix of intent recognition results.

deceptive. The BiGRU neural network could not ensure that the trained model weights were significantly different in recognizing such tactical intentions, so the final attention mechanism layer could not accurately perceive the difference in weights between them, which led to a small number of intention mutual recognition error cases.

D. COMPARATIVE ANALYSIS OF INTENTION RECOGNITION METHODS

In this experiment, the highest accuracy on the test set during 200 Epochs was selected as the accuracy of the model, whose loss was that of the model. We compared the proposed BiGRU-Attention model with the stacked auto-encoder (SAE) tactical intention intelligent recognition model of Ou *et al.* [10]; the long short-term memory (LSTM) tactical intention recognition model of the battlefield against enemy targets of Ou *et al.* [13]; a method of air combat target threat assessment based on batch normalization fully connected residual (BN-FC-RSE) network, proposed by Zhai *et al.* [11]; a study on reconnaissance target intention recognition based on radial basis function (RBF) neural network, by Wei *et al.* [12]; the deep backpropagation (DBP) neural network air target combat intention recognition model optimized using ReLU and the Adam algorithm, proposed by Zhou *et al.* [14]; the panoramic convolutional long short-term memory network (PCLSTM) for air target combat intention recognition, proposed by Xue *et al.* [15]; the traditional multi-classification model support vector machine (SVM); and multilayer perceptron (MLP). The experimental results are presented in Table2.

It can be seen from Table 3 that the proposed BiGRU-Attention model performed better than the other seven models in terms of accuracy and loss value. Its accuracy was about 30% better than those of SVM and MLP, about 20% higher than that of neural network methods that rely on single moment characteristics to recognize intention, and

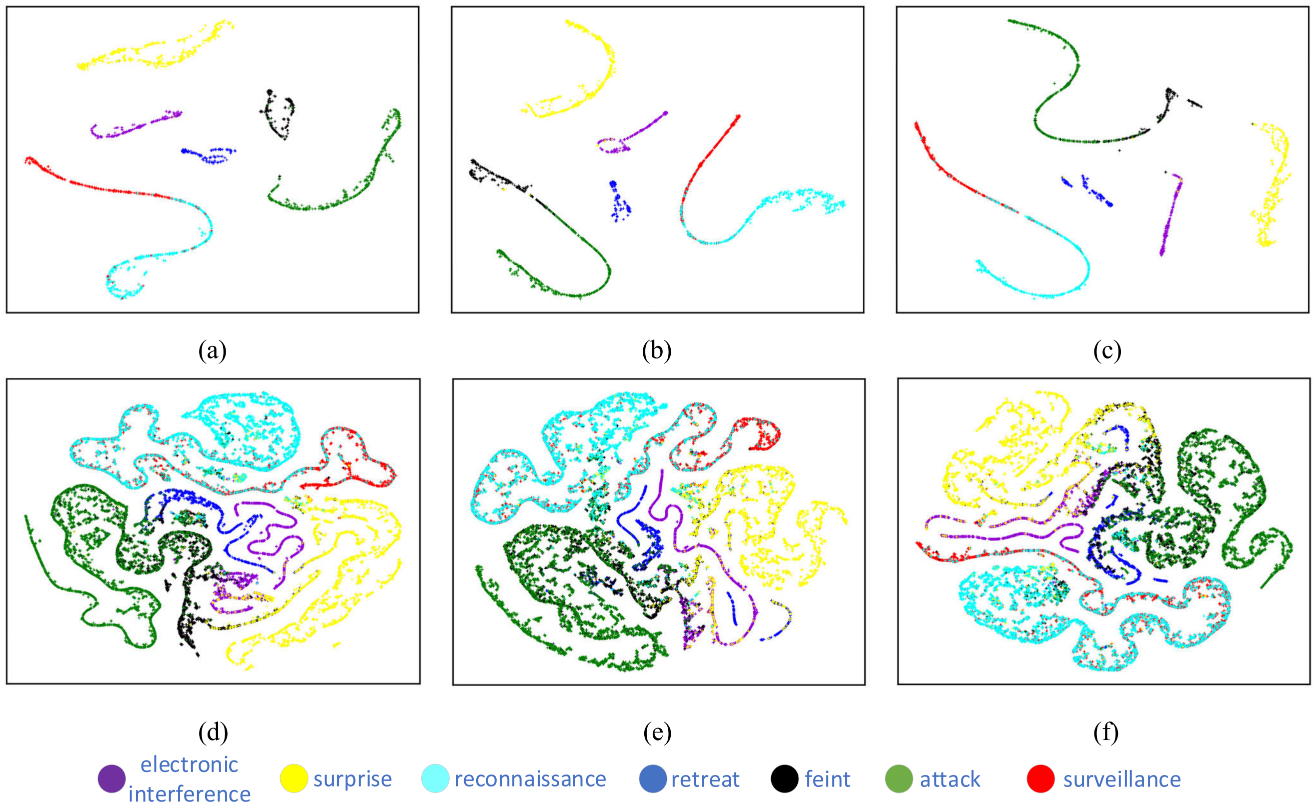

FIGURE 12. t-SNE characteristic visualization. (a) BiGRU-Attention. (b)PCLSTM. (c) LSTM. (d) BN-FC-RES. (e) SAE. (f) DBP.

TABLE 2. Intention recognition accuracy and loss of various models.

Model	Accuracy(%)	Loss
BiGRU-Attention	97.4	0.090
PCLSTM	95.9	0.109
LSTM	94.5	0.122
BN-FC-RES	82.3	0.378
SAE	78.6	0.531
DBP	77.9	0.528
RBF	73.1	0.632
MLP	70.1	0.644
SVM	68.5	0.682

2.9% better than the basic LSTM model. Compared with PCLSTM, the method of combining LSTM and CNN, our proposed method also has a good performance improvement. Further analysis indicated that LSTM, PCLSTM and BiGRU-Attention, as RNN-based temporal characteristic network models, were more suitable for air target tactical intention recognition, further demonstrating that it is more scientific to judge air target intentions based on temporal variation characteristics.

To investigate the discriminative properties of the characteristics extracted by different intention recognition methods, we utilize the t-distributed stochastic neighbor embedding (t-SNE) algorithm to map extracted characteristics into two dimensions. Figure 12 compares the DBP, SAE, BN-FC-RES, LSTM, PCLSTM and the proposed BiGRU-Attention. Our proposed BiGRU-Attention is significantly better than the other five intention recognition methods in distinguishing between attack intention and feint intention. At the same time, our proposed method has short intra-class distances and long inter-class distances, indicating that its characteristic extraction effect is better, and the classification effect is easier to achieve. It can make full use of the advantages of each component structure to improve the performance of intent recognition.

E. COMPARATIVE EXPERIMENT WITH BILSTM-ATTENTION MODEL

This paper compares the intention recognition model of BiGRU-Attention with that of BiLSTM-Attention, and further explains why GRU network is chosen to replace LSTM network. The results are shown in Table 3 and Figure 13. By comparing the accuracy, loss, and average time of the two models, it can be concluded that the GRU network is simpler than LSTM network structure in the case of similar performance, which makes the BiGRU-Attention model have a lower time complexity. Meanwhile, for the 0.5s sampling interval of air combat characteristics, the 0.368ms intention recognition duration can provide the enemy intention in time.

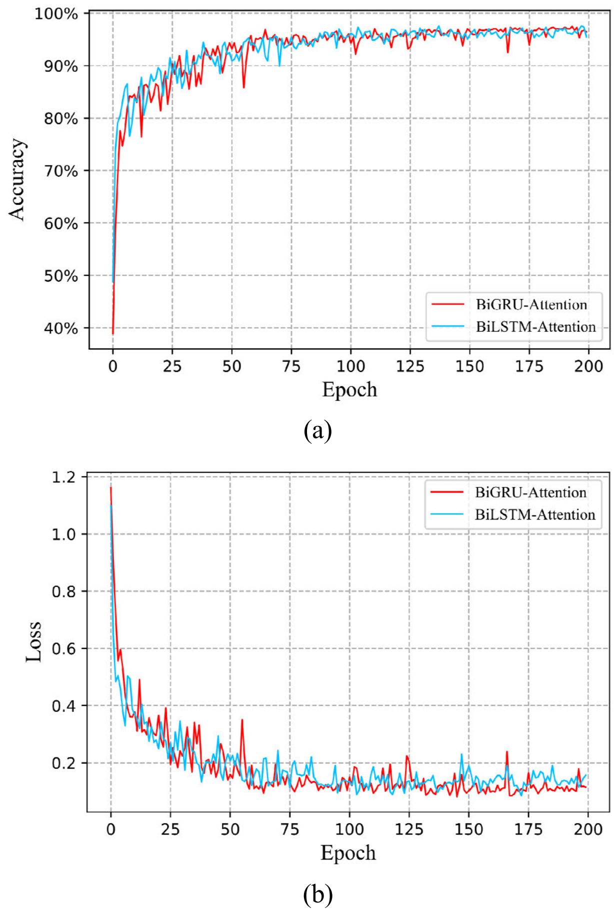

FIGURE 13. Experimental results of two models. (a) Accuracy comparison. (b) Loss comparison.

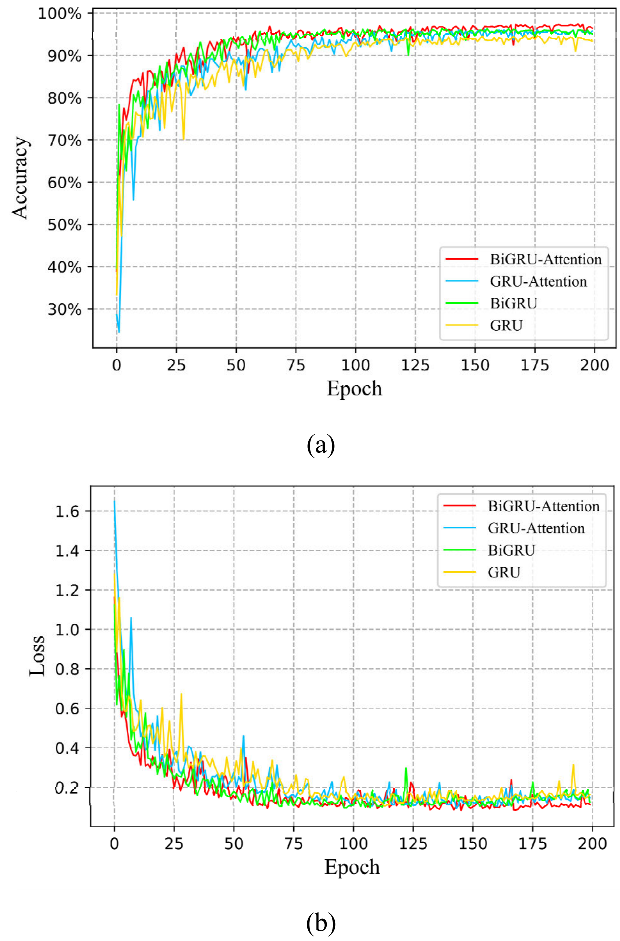

FIGURE 14. Ablation experiment results. (a) Model ablation experiment accuracy. (b) Model ablation experiment loss.

TABLE 3. Bigru-Attention model and Bilstm-Attention model intention recognition results.

Model	Accuracy(%)	Loss	Time(ms)
BiGRU-Attention	97.4	0.090	0.368
BiLSTM-Attention	97.3	0.087	0.394

TABLE 4. Results of ablation experiments.

Model composition structure			Accuracy(%)	Loss
Bidirectional	GRU	Attention		
√	√	√	97.4	0.090
√	√		96.3	0.100
	√	√	96.2	0.101
	√		94.9	0.115

F. ABLATION EXPERIMENT

Although the comparison of BiGRU-Attention model with PCLSTM, LSTM, BN-FC-RES, SAE, DBP, RBF, MLP, and SVM models have fully demonstrated that the BiGRU-Attention model could accurately identify the air targets tactical intention with high accuracy and low loss, it does not belong to the comparison of the same type of mixed experimental models. Therefore, we conducted model ablation experiments on the same dataset, with results as shown in Table 4, Figure 14.

It can be seen from Table 4 that the accuracy of the proposed model could reach 97.4%. Compared to GRU, GRU-Attention, and BiGRU, the accuracy of BiGRU-Attention was better by 2.5%, 1.2%, and 1.1%, respectively. Its loss was lower than those of the other three models. From the analysis of the changes in accuracy and loss of the ablation experiments in Figure 10, the overall accuracy of the four models increased and the loss decreased with the increase of training epochs, and the BiGRU-Attention model is better than the other three models. The BiGRU-Attention and BiGRU models converge around the 60th round, and the GRU-Attention and GRU models converge around the 80th round. The convergence speed of BiGRU-Attention and BiGRU models is significantly better than the other two models. After analysis, the bidirectional propagation mechanism can effectively improve the network learning effect, so that the neural network model can learn faster under the same batch size, learning rate, and the number of neurons.

TABLE 5. Results of evaluation indexes of ablation experiment.

Intention Type \ Evaluation Index	Precision(%)				Recall(%)				F1 Score			
	①	②	③	④	①	②	③	④	①	②	③	④
Attack	98.6	98.1	98.3	96.7	97.0	95.8	95.8	93.8	0.978	0.970	0.970	0.953
Reconnaissance	97.4	96.7	96.6	95.1	94.9	94.4	94.2	93.7	0.961	0.955	0.954	0.944
Feint	93.8	89.4	88.2	84.3	98.0	97.0	97.0	94.0	0.956	0.930	0.923	0.889
Surveillance	92.2	90.1	90.4	90.0	96.1	95.3	95.3	93.8	0.940	0.930	0.923	0.918
Surprise	99.7	99.0	99.2	98.7	99.0	97.0	96.8	96.3	0.992	0.980	0.980	0.975
Retreat	100	100	100	100	100	100	100	100	1	1	1	1
Electronic interference	99.5	99.0	99.0	98.3	99.5	97.3	97.3	96.2	0.992	0.981	0.981	0.973

The convergence curves of the BiGRU and GRU-Attention models are relatively close, and both are significantly better than the GRU model. It can be seen that the introduction of bidirectional propagation and attention mechanisms could significantly improve the GRU model.

The precision (ratio of the number of correctly identified positive samples to the number of positive samples), recall (ratio of the number of correctly identified positive samples to the actual number of positive samples), and F1 score (harmonic mean of precision rate and recall rate) were used to further validate the model. The results are shown in Table 5.

Table 5, ①, ②, ③, and ④ respectively represent the BiGRU-Attention, BiGRU, GRU-Attention, and GRU air target tactical intention recognition models. It could be concluded that the four models have relatively low recognition rates for feints and surveillance intentions, which, after analysis, should be due to the high similarity of air combat characteristics between these two intentions and the attack and reconnaissance intentions. The recognition rates were relatively higher for retreat intentions. The differences between the results of the three evaluation indicators of the BiGRU and GRU-Attention models were smaller but significantly higher than those of GRU. The BiGRU-Attention model was superior on all evaluation indicators, which shows that it can recognize air target tactical intentions with high accuracy.

G. HUMAN BEHAVIOR RECOGNITION

Because the air combat intent data set used in this article cannot be made public. Therefore, we used the public human behavior recognition data set to further verify the proposed model. The data set comes from the "Activity Recognition system based on Multisensor data fusion (AReM)" in the UC Irvine Machine Learning Repository. This dataset contains temporal data from a Wireless Sensor Network worn by an actor performing the activities: bending, cycling, lying down, sitting, standing, walking. The collection time of each action lasts for 120 seconds, and the sampling interval is 250 milliseconds. The human behavior data set was processed according to the sample construction method in this article, and a total of 3,520 samples were constructed. Divide the training set and the test set according to 8:2, and input the test set into the models to get the results shown in Table 6.

TABLE 6. Behavior Recognition Accuracy and Loss of Various Models.

Model	Accuracy(%)	Loss
BiGRU-Attention	98.2	0.069
PCLSTM	96.5	0.103
LSTM	93.8	0.161
BN-FC-RES	83.4	0.368
SAE	76.6	0.560
DBP	80.9	0.468
RBF	76.2	0.585

It can be seen from Table 6 that our proposed model still performs well in the recognition of human behavior intentions, with the highest accuracy rate and the lowest loss value. At the same time, it further proves that the method of inferring intentions at multiple moments is more accurate than making judgments at a single moment.

H. STATISTICAL TEST

In order to accurately evaluate the proposed method, we refer to the method in References [32], [33] to test the statistical significance of the two data sets. We used the two-tailed T-tests method to analyze the significance of the two index results obtained by the proposed model to verify that the results we obtained were not obtained by accident. The calculation formula is as follows:

$$\bar{x} = \frac{1}{n}\sum\nolimits_{i=1}^{n} \hat{x}_i \tag{15}$$

$$s = \sqrt{\frac{\sum_{i=1}^{n}\left(\hat{x}_i - \bar{x}\right)}{n-1}} \tag{16}$$

$$t = \sqrt{n}\left|\frac{\bar{x} - x_{max}}{s}\right| \tag{17}$$

Take the calculation of the statistically significant difference in the loss value of Our Dataset as an example. First, use formula (15) to calculate the average of the 10 results of the test Loss value as $\bar{x}$ =0.0900 ($m = 10$, $\hat{x}_i$ represents the i-th test Loss value). Then, use formula (16) to calculate the standard deviation of the Loss value as $s = 0.0031$. Finally, use formula (17) to calculate the critical value as $t =$ 4.049 (x_{max} =0.0940 is the assumed maximum Loss value).

TABLE 7. Hypothesis test result.

Metrics / Datasets	Accuracy			Loss		
	x_{min}	t	1-α	x_{max}	t	1-α
Our Dataset	0.970	3.911	0.99	0.0940	4.049	0.99
AREM	0.975	12.81	0.999	0.0730	4.549	0.998

By comparing the two-tailed T-test table, 4.049>3.250 can be obtained. Therefore, our proposed model test Loss value is less than the assumed maximum value of 0.094, which has a confidence degree of (1-α =0.99). The remaining experimental results are shown in Table 7.

According to the statistical results in Table 7, we can see that the minimum value of our assumed accuracy is greater than the maximum value of other comparison methods, and the maximum value of the assumed loss value is less than the minimum value of other comparisons methods. Therefore, there is a statistically significant difference between our proposed model and other comparison methods, which is significantly better than other comparison methods.

V. CONCLUSION

In a complex battlefield environment, it is difficult to efficiently identify enemy target intentions based only on expert experience. Traditional air target tactical intention recognition is based only on single moment analysis, which lacks a scientific basis and has low accuracy. We analyzed the characteristics of the air combat target tactical intention recognition problem, adopted a hierarchical strategy to select 17-dimensional air combat characteristics from both threat levels and combat missions, encapsulated the cognitive experience of decision-makers as labels, and proposed the BiGRU-Attention air combat target tactical intent recognition model utilizing the variation of air target temporal characteristics. The model used a BiGRU neural network to fully learn 12 consecutive frames of air combat characteristic information to extract deeper characteristics, and applied an attention mechanism to assign weights to the characteristics for more precise intention recognition. Results of comparative experiments showed that the proposed model learned faster and had higher recognition accuracy. In addition, because the current research is to set labels artificially, the computer will inevitably recognize the error when the experts in the air combat field judge the enemy's intentions incorrectly. How to make computers more accurate than experts in the field of air warfare in the recognition of tactical intention of air targets, rather than just the recognition speed, will be the focus of our next research. We initially intend to use unsupervised clustering methods for research.

REFERENCES

[1] Z. D. Liu, M. Chen, and Q. Wu, "Prediction of unmanned aerial vehicle target intention under incomplete information," (in Chinese), *Sci. Sinica Informat.*, vol. 50, no. 5, pp. 704–717, Apr. 2020, doi: 10.1360/SSI-2019-0106.

[2] F. J. Zhao, Z. J. Zhou, C. H. Hu, L. Wang, and T. Y. Liu, "Air target intention recognition method based on confidence rule base and evidential reasoning," *Electroopt. Opt. Control*, vol. 24, no. 8, pp. 15–19 and 50, 2017.

[3] X. T. Li, "The research and implementation of situation assessment in the target intention recognition," M.S. thesis, North Univ. China, Taiyuan, China, 2012.

[4] X. Yin, M. Zhang, and M. Q. Chen, "Combat intention recognition of the target in the air based on discriminant analysis," *J. Projectiles, Rockets, Missiles Guid.*, vol. 38, no. 3, pp. 46–50, 2018, doi: 10.15892/j.cnki.djzdxb.2018.03.011.

[5] J. Qing, G. Xiantai, J. Weidong, and W. Nanfang, "Intention recognition of aerial targets based on Bayesian optimization algorithm," in *Proc. 2nd IEEE Int. Conf. Intell. Transp. Eng. (ICITE)*, Piscataway, NJ, USA, Sep. 2017, pp. 356–359, doi: 10.1109/ICITE.2017.8056938.

[6] Y. Song, X.-H. Zhang, and Z.-K. Wang, "Target intention inference model based on variable structure Bayesian network," in *Proc. CiSE*, Wuhan, China, Dec. 2009, pp. 333–340, doi: 10.1109/CISE.2009.5365659.

[7] X. U. Ximeng, Y. Rennong, and F. U. Ying, "Situation assessment for air combat based on novel semi-supervised naive Bayes," *J. Syst. Eng. Electron.*, vol. 29, no. 4, pp. 768–779, Aug. 2018, doi: 10.21629/JSEE.2018.04.11.

[8] N. F. Wu, "Research on cluster intention recognition method based on recurrent neural network," M.S. thesis, Southwest Jiaotong Univ., Chengdu, China, 2019.

[9] T. Zhou, M. Chen, Y. Wang, J. He, and C. Yang, "Information entropy-based intention prediction of aerial targets under uncertain and incomplete information," *Entropy*, vol. 22, no. 3, p. 279, 2020, doi: 10.3390/e22030279.

[10] W. Ou, S. J. Liu, X. Y. He, and S. M. Guo, "Tactical intention recognition algorithm based on encoded temporal features," *Command Control Simul.*, vol. 38, no. 6, pp. 36–41, 2016, doi: 10.3969/j.issn.1673-3819.2016.06.008.

[11] X. Y. Zhai, F. B. Yang, L. N. Ji, S. Q. Li, and S. H. Lv, "Air combat targets threat assessment based on standardized fully connected network and residual network," (in Chinese), *Fire Control Command Control*, vol. 45, no. 6, pp. 39–44, 2020, doi: 10.3969/j.issn.1002-0640.2020.06.008.

[12] W. Wei and G. B. Gongbao, "Detection and recognition of air targets by unmanned aerial vehicle based on RBF neural network," *Ship Electron. Eng.*, vol. 38, no. 10, pp. 37–40, 2018, doi: 10.3969/j.issn.1672-9730.2018.10.009.

[13] W. Ou, S. J. Liu, X. Y. He, and Z. G. Cao, "Study on intelligent recognition model of enemy target's tactical intention on battlefield," *Comput. Simul.*, vol. 34, no. 9, pp. 10–14, 2017, doi: 10.3969/j.issn.1006-9348.2017.09.003.

[14] J. Xue, J. Zhu, J. Xiao, S. Tong, and L. Huang, "Panoramic convolutional long short-term memory networks for combat intension recognition of aerial targets," *IEEE Access*, vol. 8, pp. 183312–183323, 2020, doi: 10.1109/ACCESS.2020.3025926.

[15] W. W. Zhou, P. Y. Yao, J. Y. Zhang, X. Wang, and S. Wei, "Air target combat intention recognition based on deep neural network," *Acta Aeronaut. Sinica*, vol. 39, no. 11, pp. 200–208, 2018, doi: 10.7527/S1000-6893.2018.22468.

[16] H. Chen, Q. L. Ren, Y. Hua, and Y.-N. Qiu, "Fuzzy neural network based tactical intention recognition for sea targets," (in Chinese), *Syst. Eng. Electron.*, vol. 38, no. 8, pp. 1847–1853, 2018, doi: 10.3969/j.issn.1001-506X.2016.08.20.

[17] T. H. Zhang, S. X. Peng, Q. Zou, and D. Wang, "Submarine air combat intention recognition based on unsupervised neural network," (in Chinese), *Mod. Defense Technol.*, vol. 46, no. 2, pp. 122–129, 2018, doi: 10.3969/j.issn.1001-506X.2016.08.20.

[18] G. Y. Lu and Y. Y. Ding, "Study on intention recognition to Foe of underwater platform," *Command Control Simul.*, vol. 34, no. 6, pp. 100–102, 2012.

[19] P. Xia, C. Mou, and Z. Jie, *Prediction of Air Target Intention Utilizing Incomplete Information*. Singapore: Springer, 2016.

[20] Z. F. Xi, A. Xu, Y. X. Kou, Z. W. Li, and A. W. Yang, "Target threat assessment in air combat based on PCA-MPSO-ELM algorithm," (in Chinese), *Acta Aeronaut. Astronaut. Sinica*, vol. 41, no. 9, 2020, Art. no. 323895, doi: 10.7527/S10006893.2020.23895.

[21] K. Q. Zhu and Y. F. Dong, "Study on the design of air combat maneuver library," *Aeronaut. Comput. Technol.*, vol. 31, no. 4, pp. 50–52, 2001.

[22] S. Y. Zhou, W. H. Wu, X. Li, and M. Dong, "Analysis of air combat maneuver decision set model," *Aircr. Des.*, vol. 32, no. 3, pp. 42–45, 2012.
[23] J. S. Li, W. Liang, X. M. Liu, and Z. H. Qi, "Missile midcourse target threat assessment based on maximizing dispersion," *Syst. Eng. Theory Pract.*, vol. 27, no. 5, pp. 164–167, 2007.
[24] O. Kulak, "A decision support system for fuzzy multi-attribute selection of material handling equipments," *Expert Syst. Appl.*, vol. 29, no. 2, pp. 310–319, 2005, doi: 10.1016/j.eswa.2005.04.004.
[25] X. Wang, R. N. Yang, and J. L. Zuo, "Trajectory prediction of target aircraft based on HPSO-TPFENN neural network," *J. Northwestern Polytech. Univ.*, vol. 37, no. 3, pp. 612–620, 2019, doi: 10.3969/j.issn.1000-2758.2019.03.025.
[26] X.-F. Yuan, L. Li, Y. Shardt, Y.-L. Wang, and C.-H. Yang, "Deep learning with spatiotemporal attention-based LSTM for industrial soft sensor model development," *IEEE Trans. Ind. Electron.*, vol. 68, no. 5, pp. 4404–4414, May 2021, doi: 10.1109/TIE.2020.2984443.
[27] X. Wei, L. Zhang, H.-Q. Yang, L. Zhang, and Y.-P. Yao, "Machine learning for pore-water pressure time-series prediction: Application of recurrent neural networks," *Geosci. Frontiers*, vol. 12, no. 1, pp. 453–467, Jan. 2021, doi: 10.1016/j.gsf.2020.04.011.
[28] Y. C. Sun, R. L. Tian, and X. F. Wang, "Emitter signal recognition based on improved CLDNN," *Syst. Eng. Electron.*, vol. 43, no. 1, pp. 42–47, 2021, doi: 10.3969/j.issn.1001-506X.2021.01.06.
[29] J. X. Chen, D. M. Jiang, and Y. N. Zhang, "A hierarchical bidirectional GRU model with attention for EEG-based emotion classification," *IEEE Access*, vol. 7, pp. 118530–118540, 2019, doi: 10.1109/ACCESS.2019.2936817.
[30] Y. Qiao, B. Zhang, W. Zhang, A. K. Sangaiah, and H. Wu, "DGA domain name classification method based on long short-term memory with attention mechanism," *Appl. Sci.*, vol. 9, no. 20, p. 4205, Oct. 2019, doi: 10.3390/app9204205.
[31] H. Zheng, F. Lin, X. Feng, and Y. Chen, "A hybrid deep learning model with attention-based conv-LSTM networks for short-term traffic flow prediction," *IEEE Trans. Intell. Transp. Syst.*, vol. 22, no. 11, pp. 6910–6920, Nov. 2021, doi: 10.1109/TITS.2020.2997352.
[32] J. Hu and W. Zheng, "A deep learning model to effectively capture mutation information in multivariate time series prediction," *Knowl.-Based Syst.*, vol. 203, Sep. 2020, Art. no. 106139, doi: 10.1016/j.knosys.2020.106139.
[33] J. Chen, Z. Gong, and W. Liu, "A nonparametric model for online topic discovery with word embeddings," *Inf. Sci.*, vol. 504, pp. 32–47, Dec. 2019, doi: 10.1016/j.ins.2019.07.048.

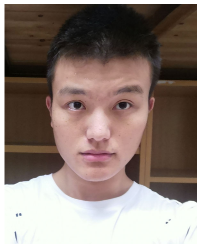

FEI TENG was born in Binzhou, Shandong, China, in 1997. He received the B.S. degree from Xiamen University, in 2019. He is currently pursuing the M.S. degree with the College of Air and Missile Defense, Air Force Engineering University. His research interests include intention recognition, intelligent information processing, and artificial intelligence.

XINPENG GUO was born in Xi'an, Shaanxi, China, in 1985. He is currently an Associate Professor with the College of Air and Missile Defense, Air Force Engineering University. His research interests include intention recognition, intelligent information processing, and artificial intelligence.

YAFEI SONG (Member, IEEE) was born in Henan, China, in 1988. He received the Ph.D. degree from Air Force Engineering University, in 2015. He has been working as a Postdoctoral Researcher with Air Force Engineering University, since April 2017, where he is currently an Associate Professor with the College of Air and Missile Defense. His research interests include intention recognition, pattern recognition, intelligent information processing, and evidential reasoning.

GANG WANG was born in Qingzhou, Shandong, China, in 1975. He is currently a Professor with the College of Air and Missile Defense, Air Force Engineering University. His research interests include intention recognition, intelligent information processing, and artificial intelligence.